

G. Brant Foote¹, Terrence W. Krauss², Viktor Makitov²
¹National Center of Atmospheric Research, Boulder, CO
²Weather Modification Inc., Fargo, ND

1. INTRODUCTION

Insurance claims due to hailstorms in urban areas have escalated over the past 10 years. A study by Herzog (2002) compiled and summarized the hailstorm damages in the USA for the period 1994-2000 for the Institute for Business and Home Safety (IBHS). Verified hail losses amounted to \$2.5 Billion per year, with the actual amount possibly being 50% higher. Insured claims from the hailstorm that struck Sydney Australia on April 14, 1999 were approximately \$1.5 billion, making it the most damaging event in Australian insurance history. And most recently, the most damaging hailstorm ever recorded in the USA moved over portions of the St. Louis and Kansas City urban areas collectively causing \$1.9 billion in damage claims from a 2-day period, becoming the ninth most costly weather catastrophe in the United States since property insurance records began in 1949 (Changnon and Burroughs, 2003). There are several reasons for making radar-hail measurements in general, and specifically for any cloud seeding project that attempts to reduce the amount and severity of the hail fall:

1. To detect hail within the cloud or on the ground (that is, hail yes/no), or estimate the probability of hail in the cell. The ability to discriminate rainstorms from hailstorms is valuable for many forecasting and scientific purposes.
2. To quantitatively estimate hail at the ground either as a point estimate at a single time, or as some quantity integrated over area and time. Examples of such metrics are: Kinetic energy flux, Mass of hail, Hail rate.
3. To study the behavior of hail metrics aloft that might be more sensitive to seeding effects in the storm.

The measurement of hail with conventional radar is a problem. The main difficulties are connected with the unknown contribution of rain to the total power that is backscattered to the radar, the size distribution of the hail, and to perhaps lesser extent the physical nature of the hailstone that affects its backscattering properties (existence of a water layer, spongy property, etc). For conventional radars, we are limited to reflectivity measurements alone, and not to various polarization or multi-wavelength measurements where the physical properties of the hail can be used to advantage for detection and measurement.

Corresponding author address: Dr. Terry Krauss, Weather Modification Inc., 3802 20th Street North, Fargo, ND USA 58102: www.weathermod.com
krausst@telusplanet.net

Although highly accurate measurements of hailfall have been claimed by some authors using reflectivity alone (for example in Switzerland), such results have generally not been found in other locations.

The idea behind looking for hail metrics aloft, relates partly to the difficulties inherent in measuring hail near the surface in the presence of rain. In addition, if seeding in fact leads to the changes in the size distribution postulated by the seeding hypothesis (more stones of a smaller size), such changes must first be evident aloft in the hail growth zone. It might be much easier to detect a seeding effect by looking in this region.

There have been arguments made since the mid 1970s that hail growth in supercell storms can be inherently different than in other storms, and that hail suppression might be more difficult. Browning and Foote (1976) argued that the presence of a weak echo region, also called a vault, was strong evidence that the natural hail process was very inefficient, and that certain dominant growth trajectories could not be eliminated even by intense seeding. Given the possibility that storms of different types and different intensities might respond differently to seeding, it is important to be able to classify storms into groups where the response is expected to be more uniform.

This paper will report on some work in progress using C-band radar data from the Mendoza, Argentina and Alberta, Canada hail suppression projects conducted by Weather Modification Inc. The sensitivity and variation with time of several radar hail parameters computed using the TITAN (Thunderstorm, Identification, Tracking, Analysis, and Now-casting) system (Dixon and Wiener, 1993) will be presented. The hail parameters are: Probability of Hail, Hail Mass Aloft, Vertical Integrated Hail Mass, Hail Kinetic Energy Flux, and an exploratory storm severity index based on the Abshaev classification scheme. The usefulness of these parameters for real-time decision-making and the evaluation of the responses to seeding are discussed.

2. CLASSIFICATION OF STORMS

It is well accepted in the literature that many types of hailstorms exist (Foote, 1985). It is possible to classify storms as supercells, multicells, squall lines, etc. Storms that form in environments with low wind shear have patterns of propagation that are often quite irregular and seemingly random. Forming in a more strongly sheared environment, supercells often evolve and move in quite regular ways. Classifying storms

based on their structural characteristics (such as those discussed by Foote and Mohr 1979, and Foote 1985) is very difficult and somewhat subjective. More recently, Abshaev has developed an objective scheme that uses only the maximum reflectivity and the height of the 45-dBZ echo, and has shown very intriguing results.

Let H_0 denote the height of the 0C isotherm, and H_{45} denote the height of the top of the 45-dBZ echo in the storm. Define $\Delta H_{45} = H_{45} - H_0$. Call Z_{max} the maximum reflectivity in the storm. Also define $\Delta Z = Z_{max} - 10$. Abshaev's four storm categories (using a 10-cm wavelength radar) are then:

- I. $Z_{max} > 15$ dBZ, and $\Delta H_{\Delta Z} \geq 2$ km.
- II. Z_{max} between 35 – 55 dBZ, and $\Delta H_{\Delta Z}$ or $\Delta H_{45} \geq 2$ km
- III. Z_{max} between 55 – 65 dBZ, and $\Delta H_{45} > 3$
- IV. $Z_{max} > 65$ dBZ, and $\Delta H_{45} > 4$ km

A new hail storm classification system presently referred to as the **FOKR** Index (for Foote-Krauss) has been implemented for use and testing with the WMI C-band radar.

- I. $Z_{max} > 40$ dBZ, above 3 km MSL (current TITAN cell tracking criteria)
- II. $Z_{max} > 45$ dBZ, above 3 km MSL
- III. Z_{max} between 45 – 55 dBZ, and $\Delta H_{45} > 3$ km
- IV. $Z_{max} > 55$ dBZ, and $\Delta H_{45} > 4.0$ km

Note that if the first echo is not high enough in altitude for Category I, then the storm is not included in this classification scheme at all. Also, since storms can evolve over time, a storm can change its category as it intensifies or weakens. In simple terms, the classification is meant to imply the following:

- Category I:** potentially hail dangerous, newly developing cumulus congestus, with first radar echo above the -8C level;
- Category II:** hail dangerous convective cells at a later stage, having a possibility of growing into hailstorms;
- Category III:** hailstorms;
- Category IV:** intense hailstorms, including supercells.

The first two categories are considered by Abshaev to be non-hailers. The second two are hailers. Category IV storms are thought to produce 5-6 times as much damage as Category III storms.

To get a unique classification for the storm, one needs to look at the Z_{max} for the whole lifetime. Note that if

there is a seeding effect that reduces (or increases) the global maximum reflectivity or height of the storm, then seeding could also bump a storm from its natural category to some other category.

3. METHODS OF DETECTING HAIL IN A STORM

In this section we consider a number of metrics using radar reflectivity factor to estimate the presence and magnitude of hail within a storm.

a. Probability of hail

Quite a lot of work has been done by scientists from the ex-Soviet Union and later by others on estimating the probability of hail from the height of the 45-dBZ contour in the storm. In the work published by Waldvogel et al. (1979), they relate ΔH_{45} to the probability of hail with S-band radars returns validated against a surface hailpad network. The results are shown in Figure 1 and Table 1, along with a third-order polynomial fitted curve. The probability of hail rises sharply as ΔH_{45} increases. One gets a hail detection scheme by thresholding on, say, $\Delta H_{45} > 2$ km (where according to Waldvogel et al. the probability of hail is only 0.2) or some higher threshold. This is discussed in detail, by Witt et al. (1998), and Kessinger and Brandes (1995) who obtained very positive results with this metric, which they called **POH**. Techniques such as this are completely heuristic, and their success in one location is no guarantee of success in another.

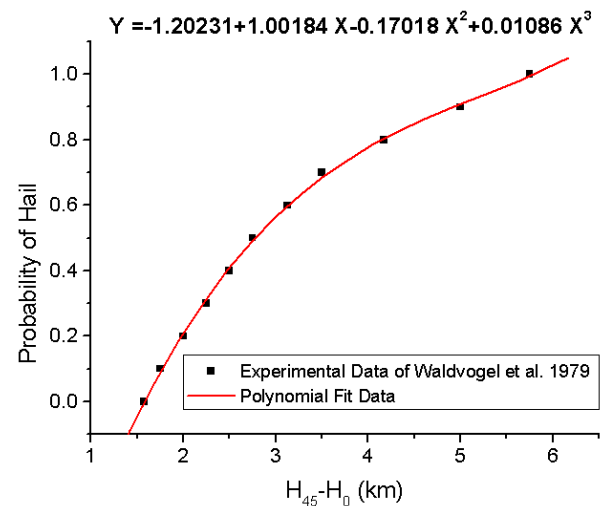


Figure 1: Probability of Hail at the surface according to height of the 45 dBZ contour above the freezing level.

Table 1: Probability of Hail at the surface according to height of the 45 dBZ contour above freezing.

HEIGHT (km)	Probability (%)
5.80	1.0
5.00	0.9
4.20	0.8
3.55	0.7
3.07	0.6
2.70	0.5
2.40	0.4
2.17	0.3
1.97	0.2
1.80	0.1
1.65	0.0

The **POH** classification presently being tested on the WMI C-band radars is based on the results of Waldvogel et al. (1979) relating the probability of hail falling at the surface as a function of the maximum height of the 45 dBZ contour above freezing, according to the values shown in Table 1.

b. Kinetic energy flux

Kinetic Energy (KE) flux at the surface is computed only for positions (columns) for which two conditions are met (illustrated in Figure 2):

- a. $Z > 55$ dBZ at the surface, and
- b. $Z > 45$ dBZ at height > 2 km above the OC level

The KE flux is computed using the relation:

$$KE = 5.0 \times 10^{-6} Z^{0.840} \quad (\text{J m}^{-2} \text{s}^{-1})$$

c. Hail mass aloft (G_A)

In looking for a more sensitive measure than the volume of a Z-contour, it seems that one could do better by looking at the actual reflectivities in the volume $Z > 55$ dBZ. However, for C-band radar these reflectivities are less common and, therefore, the 45 dBZ threshold is used for the WMI operational radars in Mendoza and Alberta. If there are microphysical changes from seeding, there should be changes within this high reflectivity region. In order to make the units of a volume integral physically meaningful, it is suggested that the metric should be the total estimated hail mass G_A (ktons) aloft, rather than an integral of Z itself. **Total hail mass aloft** is computed using the following:

$$G_A = \int_{Z>45} \int_{H>H_2} M \, dV$$

where M (g m^{-3}) is a function of reflectivity at each range gate (see below) and the integration is done over the TITAN cell for reflectivity >45 dBZ at heights >2 km above the OC level. This should be capable of detecting

intensity changes that wouldn't necessarily affect the volume of some reflectivity contour itself.

The hail mass, M , is computed using the following relation:

$$M = 2.32 \times 10^{-5} Z^{0.706} \quad (\text{g m}^{-3})$$

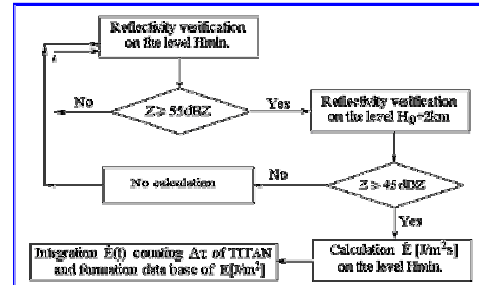
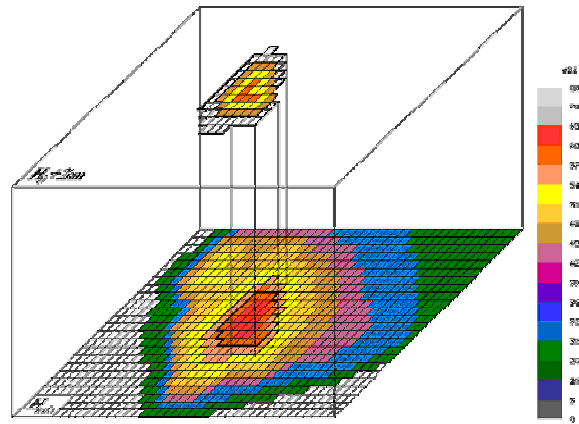


Figure 2: Schematic figure showing how Kinetic Energy Flux is computed only for positions (columns) for which two conditions are met

d. Hail mass flux at the surface (\dot{G})

The hail mass flux at the surface is computed in a similar manner to the KE flux except that it ignores the condition aloft but it uses the same threshold at the lower altitude, i.e.: $Z > 55$ dBZ at the surface.

The hail mass flux is computed using:

$$\dot{G} = 6.53 \times 10^{-4} Z^{0.747} \quad (\text{mm hr}^{-1})$$

e. Vertically integrated hail mass

The Vertical Integrated Hail Mass (**VIHM**) is computed for the entire cell (not for each point over the ground). The calculation is done the same way as VIL calculations that use the maximum reflectivity at each level within a cell, but using the reflectivity conversion to hail mass

rather than the rain relationship. As with VIL_{max} , by using the maximum reflectivity at each height $VIHM$ becomes an upper estimate of the integrated hail mass within the cell defined by the TITAN software.

4. DISCUSSION

WMI has used **POH** as a cell annotation in TITAN during cloud seeding operations as a decision-making tool to help decide which storm cells should be given priority in seeding. The **POH** has proven to be useful by combining several important storm properties (max reflectivity and vertical distribution of the reflectivity) into one simple index.

A comparison of a crop damage survey map in Mendoza with the swath of kinetic energy flux (the swath shows the maximum **KE** that occurred at each point as the storm passed over) for the severe hailstorm on 1-March-2003 is shown in Figure 3. There is relatively good agreement regarding the aerial extent of the damage and locations of several local maxima between the two maps. An area of damaging hail extending outside the agricultural zone is shown in the radar **KE** map.

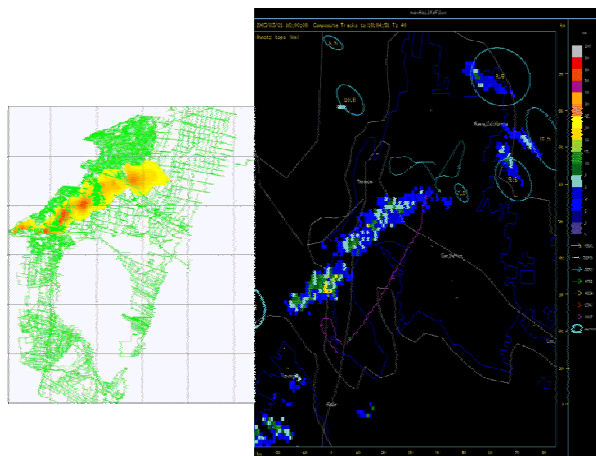


Figure 3: Comparison of the Crop Damage survey map (left, provided by the DPC, Gov. of Mendoza) with TITAN maximum kinetic energy flux (right) for the severe hailstorm on 1-March-2003.

The radar KE flux has also proven to be a good discriminator of damaging hail in Alberta. A max reflectivity map for a storm on August 24, 2004 is shown in Figure 4. The corresponding max KE flux map is shown in Figure 5. The storm was a long-lived severe storm with continuous regions of high reflectivity. The max KE flux map shows the much smaller, isolated regions that corresponded well with surface reports of large damaging hail, especially for the region 25 km east of Calgary.

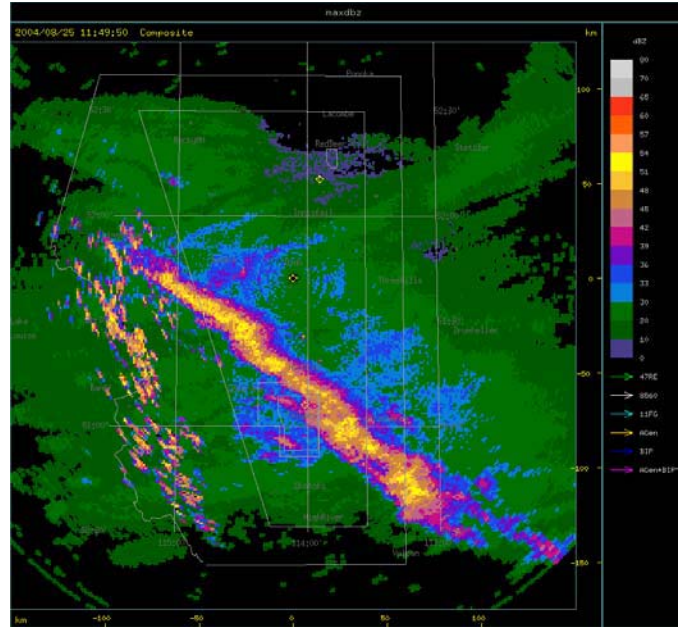


Figure 4: Maximum reflectivity map for August 24th, 2004.

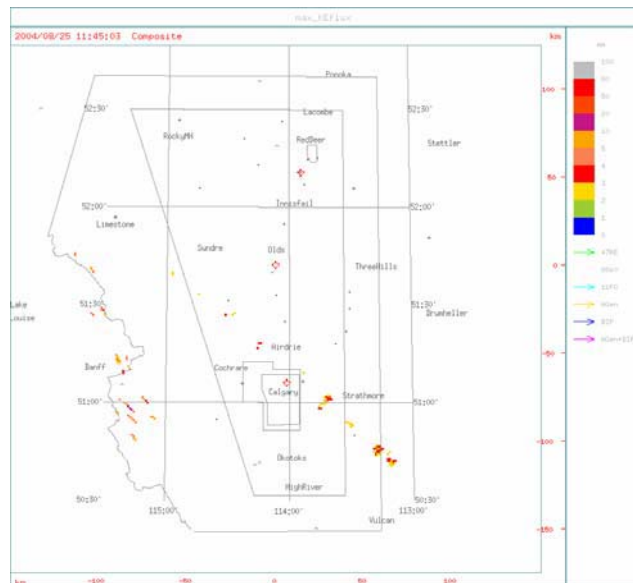


Figure 5: Maximum Kinetic Energy Flux map for August 24th, 2004.

The time history plots of **VIHM**, hail mass aloft (G_A), Probability of Hail (**POH**), and the **FOKR** index for a severe, long-lived hail storm that occurred in Alberta on 15-July-2004 is shown in Figure 6. Early in the cell lifetime (1900 to 2100) the **POH**, **VIHM**, and G_A fluctuate greatly. After 2200Z, the **POH** = 1 and G_A shows more variation than the **VIHM**. Around 0200Z, the **FOKR**

index reaches **Category III** for an extended period of time, which corresponds to the highest values of **VIHM** and **G_A**. Both **VIHM** and **G_A** could be more sensitive to cloud seeding based on these preliminary observations.

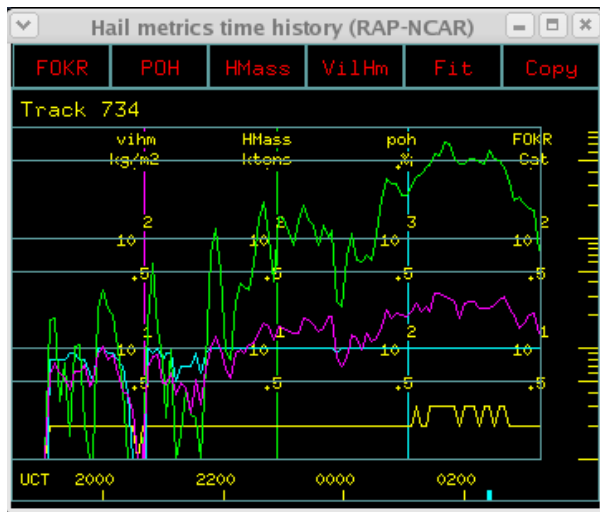


Figure 6: Time history of hail metrics (VIHM in purple, G_A in green, POH in cyan, FOKR in yellow) for a severe storm in Alberta on 15-July-2004.

Many severe storms occurred on January 22-23, 2004 in Mendoza. The new hail metric parameters of TITAN were analyzed to see what the differences were between the seeded and non-seeded storms on these two days. The data set consists of 216 cell measurements from 23 storms (complex-cells) that were “seeded”, and 1091 cell measurements from 76 storms (complex-cells) that were “non-seeded”.

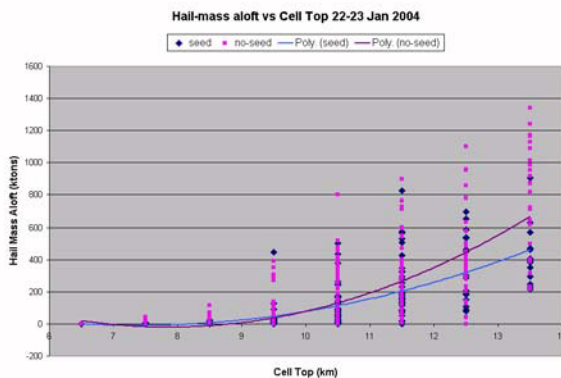


Figure 7: The Mass of hail aloft (ktons) according to cell top height (km) of 216 seeded and 1091 non-seeded cells on January 22-23, 2004.

The Mass of hail aloft, **G_A**, as a function of cell top height for all seeded and non-seeded cells on January 22-23, 2004 is shown in Figure 7. The polynomial fitted curves show a tendency toward less hail mass aloft for seeded cells than non-seeded cells of the same height

for tops >10.5 km, and little or no difference when cell top heights were <10.5 km.

The Mass of hail aloft (**G_A**) as a function of time after seeding for 293 seeded cell observations from 12 seeded storms on Jan 22-23, 2004 is shown in Figure 8. The polynomial fitted curve indicates that the mass of hail aloft starts decreasing (on average) soon after the start of seeding. The figure also shows that the hail mass aloft decreases substantially by 30 min after the start of seeding. These data may suggest the existence of a seeding effect that is most apparent 30 min after the start of seeding. However, other interpretations are possible, and one needs to compare this behavior with that of natural (unseeded) storms to be more definitive.

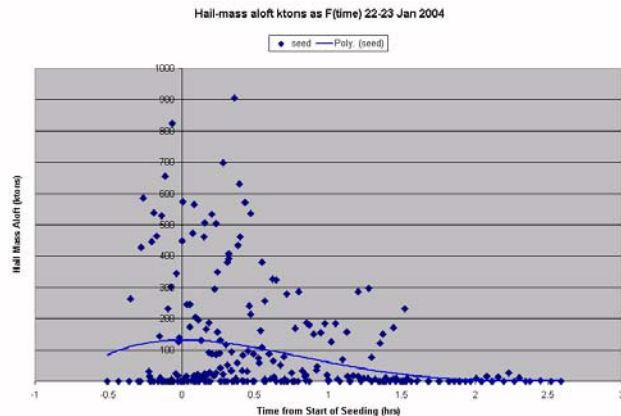


Figure 8: Mass of hail aloft (ktons) as a function of time (hours) after seeding onset (t_0) for all seeded cells on Jan 22-23, 2004.

In reality, there is some arbitrary time t_0 in the lifetime of a storm where an operational program starts seeding it. This may be, for example, after it crosses the boundary of a target zone, or when an aircraft first arrives at the storm to begin seeding. Note that in many cases there is already hail aloft at this time according to the **G_A** metric. Such a result is unavoidable in practical terms. Techniques for selecting, in an unbiased way, comparable unseeded storms, and for defining a comparable t_0 for them, need to be developed in order to properly compare seeded and control samples in a search for seeding effects.

5. CONCLUDING REMARKS

The new hail metrics have shown skill at delineating regions of the most damaging hail and in providing more information regarding the vertically-integrated intensity of a storm into a single parameter. The hail mass aloft (**G_A**) has been shown to be sensitive to subtle changes in storm structure and character. Further testing will be conducted to see if there are detectable and consistent changes in these metrics as a result of cloud seeding, and whether the new hail metrics can be used to stratify storms into different categories that may respond differently to seeding.

Acknowledgements: The authors wish to thank the following: Mr. Patrick Sweeney, President of WMI, for support of the scientific studies and software development; The Ministry of Economy, Government of Mendoza, for their support of the operational hail program and surface hail damage surveys; Mr. Jim Renick and the Alberta Severe Weather Management Society for their support; Dr. Mike Dixon, Ms. Terri Betancourt and Dr. Sue Dettling of the National Center for Atmospheric Research for incorporating the hail metrics into the TITAN radar processing software.

REFERENCES

- Abshaev, M. T., 1999: Evolution of seeded and non seeded hailstorms. Proc. Seventh WMO Scientific Conf. On Wea. Modification. WMP Report No. 31, World Meteorological Organization, Geneva, 407-410.
- Browning, K.A., and G.B. Foote, 1976: Airflow and hail growth in supercell storms and some implications for hail suppression. *Quart. J. Roy. Met. Soc.*, 102, 499-534
- Changnon, S.A., J. Burroughs, 2003: The Tristate Hailstorm: The Most Costly on Record. *Monthly Weather Review*: 131 (8), pp. 1734-1739
- Dixon, M., and G. Wiener, 1993: TITAN: Thunderstorm Identification, Tracking, Analysis, and Nowcasting - A Radar-based Methodology. *J. Atmos. and Oceanic Technol.*, 10, 6, 785-797.
- Foote, G.B., 1984: The study of hail growth utilizing observed storm conditions. *J. Climate. Appl. Meteor.*, 23, 84-101.
- Foote, G. B., 1985: Aspects of cumulonimbus classification relevant to the hail problem. *J. Rech. Atmos.*, 19, 61--74.
- Foote, G. B. and C. G. Mohr, 1979: Results of a randomized hail suppression experiment in northeast Colorado. Part VI: Post hoc stratification by storm type and intensity. *J. Appl. Meteor.*, 18, 1589-1600.
- Herzog, R., 2002: Hailstorm Loss Database 1994-2000. Institute for Business and Home Safety Annual Congress. Nov. 2000, Tampa Fl.
- Kessinger, K. J., and E. Brandes, 1995: A comparison of hail detection algorithms. Summary report to FAA, NCAR, Boulder, 52 pp.
- Waldvogel, A., Schmid, and B. Federer, 1978: The kinetic energy of hailfalls. Part I: Hailstone spectra. *J. Appl. Meteor.*, 17, 515-520.
- Waldvogel, A., B. Federer, and P. Grimm, 1979: Criteria for the detection of hail cells. *J. Applied Meteor.*, 25, 1521 -1525.
- Witt, A., M. Eilts, G. Stumpf, J. Johnson, E. deWayne, and K. Thomas, 1998: An enhanced hail detection algorithm for the WSR-88D. *Weather and Forecasting*, 13, 286-303.